J|A|C|S COMMUNICATIONS

Published on Web 09/22/2010

Stimuli-Responsive Smart Gels Realized via Modular Protein Design

Tijana Z. Grove,[†] Chinedum O. Osuji,[‡] Jason D. Forster,[§] Eric R. Dufresne,[‡,§,||,⊥] and Lynne Regan*[,†,#]

Departments of Molecular Biophysics and Biochemistry, Chemical and Environmental Engineering, Mechanical Engineering and Materials Science, Physics, Cell Biology, and Chemistry, Yale University, New Haven, Connecticut 06511, United States

Received July 26, 2010; E-mail: lynne.regan@yale.edu

Abstract: Smart gels have a variety of applications, including tissue engineering and controlled drug delivery. Here we present a modular, bottom-up approach that permits the creation of protein-based smart gels with encoded morphology, functionality, and responsiveness to external stimuli. The properties of these gels are encoded by the proteins from which they are synthesized. In particular, the strength and density of the network of intermolecular cross-links are specified by the interactions of the gels' constituent protein modules with their cognate peptide ligands. Thus, these gels exhibit stimuli-responsive assembly and disassembly, dissolving (or gelling) under conditions that weaken (or strengthen) the protein−peptide interaction. We further demonstrate that such gels can encapsulate and release both proteins and small molecules and that their rheological properties are well suited for biomedical applications.

Harnessing proteins to create smart gels with an array of applications, including tissue regeneration scaffolds and controlled drug delivery devices, has been much anticipated.[1−10] The gel designs we present are based on the 34 amino acid tetratricopeptide repeat (TPR).[11] The modular construction of repeat proteins allows many different permutations and combinations of their constituent modules to be rapidly created and tested. Moreover, additional modules can be readily incorporated to introduce additional functions, such as cell-specific binding. Natural TPR domains facilitate the assembly of macromolecular complexes, held together by specific TPR−peptide interactions.[12]

The TPR adopts a helix−turn−helix structure, which in tandem arrays forms a rigid superhelix with eight repeats per superhelical turn (Figure 1 A,B). The properties of individual TPR units can be manipulated, and the stability of arrays of TPRs can be predicted on the basis of their constituent units.[13−16] TPR modules can be engineered to bind different peptide ligands. Such binding is highly specific, and a variety of TPR modules with different binding specificities and affinities have been created in our laboratory.[17−22] Individual TPR units can thus be mixed and matched in a modular fashion to create proteins of predictable structure, stability, and function. Consequently, TPR arrays show tremendous promise for the assembly of biomaterials with an unprecedented degree of tunability. Moreover, the TPR−peptide interaction is robust in the presence of nonspecific proteins, for example, mock serum 7% BSA (K. Lai, R. Collins, T. Z. Grove, L. Regan, unpublished data).

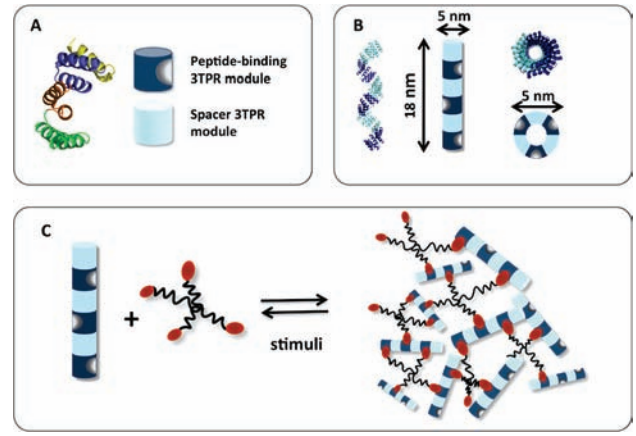

Figure 1. Modularity of TPR proteins allows the design of smart gels with predetermined structures. (A) Ribbon and cartoon representations of the structure of the 3TPR module used as either a spacer or a binding unit in the gel designs (based on PDB 1NA0). Each component 34 amino acid repeat is shown in a different color in the ribbon representation. The thermodynamic stability of both the spacer and binding modules can be varied greatly, from a melting temperature of less than 37 °C to over 100 °C.[11,14] The specificity and affinity of the binding module can also be manipulated. (B) Ribbon and cartoon representations of the structure of an 18TPR array, side and end on views (based on PDB 2FO7).[16] The 3TPR modules are colored as in panel A. The superhelical rise is 1 nm per repeat, and 8TPR repeats form one turn of the superhelix. The 18TPR array is 18 nm long, with an outer diameter of 5 nm. (C) Cartoon representation of TPR gel formation. The PEG−peptide cross-linker is represented by black lines for the PEG component and red ovals for the peptide. The cartoon is drawn approximately to scale; each arm of the 10 kDa four-arm star PEG has a contour length of ∼18 nm.

In our strategy, TPR arrays are cross-linked by multivalent peptide ligands[23,24] to create percolating three-dimensional networks (Figure 1C). Specifically, the TPR protein incorporates both peptide-binding and "spacer" 3TPR modules, arrayed along the superhelix such that the cross-linking is specific and directional and inter-protein cross-links are favored (Figure 1B).

Upon mixing the TPR array and the PEG−peptide component, self-supporting hydrogels form spontaneously at room temperature (Figure 2A). Gelation does not require chemical cross-linking reagents, redox chemistry, or extreme conditions, all of which could preclude *in vivo* applications.[6,10]

Here, we present the characterization of gels formed from 1 wt /vol% TPR in aqueous solution, with a 1:2 ratio of TPR−peptide binding sites to peptide units (Figure 2). The resultant gels are cross-linked by specific noncovalent interactions between binding modules of the repeat protein and their peptide ligands. Because such interactions are intrinsically reversible, gelation is also reversible under conditions determined by the nature of the protein−peptide interaction. The kinetics of gel formation depend on the concentra-

[†] Department of Molecular Biophysics and Biochemistry.
[‡] Department of Chemical and Environmental Engineering.
[§] Department of Mechanical Engineering and Materials Science.
[||] Department of Physics.
[⊥] Department of Cell Biology.
[#] Department of Chemistry.

 10.1021/ja106619w

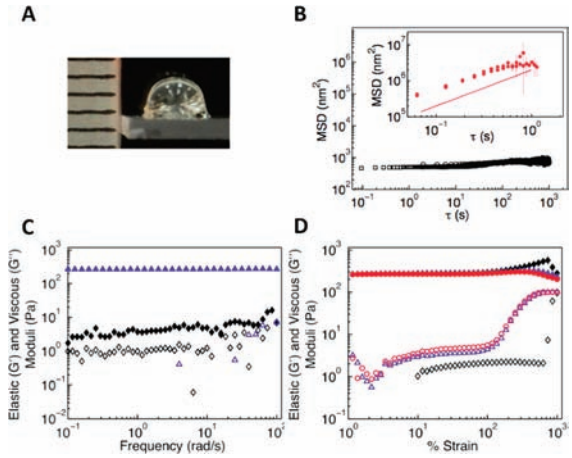

Figure 2. TPR-based smart gels are self-supporting, soft yet elastic materials. (A) Photograph of a gel cast in the bottom of a microcentrifuge tube. A ruler is shown alongside for scale: 1 tic corresponds to 1 mm. (B) Microrheology measurements tracking the Brownian motion of fluorescent probe particles. The mean-squared displacement is plotted as a function of time. The data for individual gel components are shown as red squares, with a line of slope = 1 drawn for comparison. The data for the gel, 21 days post mixing, are shown as open black squares. (C) Frequency dependence of the elastic modulus (G', closed symbols) and the viscous modulus (G'', open symbols). Behavior at the onset of gelation (diamonds, 243 h post mixing) and close to the end of gelation (triangles, 292 h post mixing) is shown. Defining characteristics of a gel are that (i) the value of G' is independent of frequency and (ii) the value of G' is larger than that of G''. Both of these conditions are clearly met by the TPR smart gels. (D) Iterative strain sweeps (black, blue, red in order of acquisition): elastic modulus (G', solid diamonds) and viscous modulus (G'', open diamonds). The strain-hardening followed by yielding at 1000% strain is evident. The elastic modulus recovers to its initial value after repeated strain sweeps.

tion of the components, the ratio of TPR−peptide binding domains to peptides, and solution conditions. Detailed phase diagrams and kinetic studies of gelation will be presented elsewhere.

We characterized the viscoelastic properties of the gels using both microrheology and bulk rheology. In microrheology measurements, we tracked the Brownian motion of 100 nm radius fluorescent probe particles.[25] The TPR or peptide solutions alone (or the mixture immediately post mixing) display liquid-like behavior, with the probe particles moving freely (Figure 2B). By contrast, after gelation, the probe particles become trapped in the gel, and their mean-squared displacement is independent of time across the range of time scales observed. Thus, the material entraps the probe particles and is actually too strong for us to accurately estimate the storage and loss moduli in this experimental setup. In bulk rheology measurements,[26] gelation is evidenced by the emergence of a frequency-independent elastic modulus (G', Figure 2C). Initially, the mixture of the TPR and peptide components exhibits liquid-like behavior, with an elastic modulus too small to be effectively measured (<∼5 Pa). Upon gelation, the elastic modulus increases to 270 Pa, comparable to the elastic modulus of a gel made of 15% Jell-O gelatin or 5% polyacrylamide/bisacrylamide.[27] An elastic modulus of 270 Pa is more than sufficient to maintain mammalian cells in suspension for tissue regeneration applications, the minimum requirement for which has been estimated as 50−100 Pa.[9,28]

The gel exhibits a remarkably large, linear viscoelastic regime and can be stretched 10 times its thickness before it yields. Upon relaxation it recovers its elasticity and can be stretched and relaxed repeatedly (Figure 2D). Such high yield-strains are unprecedented for noncovalently cross-linked polymer and biopolymer gels. Interestingly, the gel displays a modest strain stiffening in advance of yielding, likely due to the finite extensibility of the PEG−peptide cross-linker. While it is generally not observed in synthetic polymer gels, strain stiffening is a nearly ubiquitous feature in the rheology of many biological materials, where it aids in the prevention of excessive deformations.[29] The rheological properties that our gels exhibit are well-suited for biological applications that require soft yet elastic media with good mechanical integrity.[30]

There are many ways in which to incorporate stimuli responsiveness into TPR-based gels. The gel design we present here is cross-linked by the specific noncovalent interaction of the peptide DESVD-COO^- with a specific TPR binding unit. This interaction is predominantly electrostatic, and thus its strength decreases as the ionic strength increases. Specifically, in 10 mM NaCl, the dissociation constant of the peptide−TPR interaction is 5 μM, and this value decreases to 300 μM when the salt concentration is increased to 500 mM. Therefore, these gels erode in high salt. Figure 3a shows the time course of erosion of gels placed in solutions of different ionic strengths. The higher the concentration of salt, the faster the gel dissolves. This process is reversible: when the salt concentration is decreased, the gel re-forms.

A desirable property of smart materials, related to their potential application in drug delivery, is the ability to encapsulate and subsequently release entrapped materials. To test the ability of these

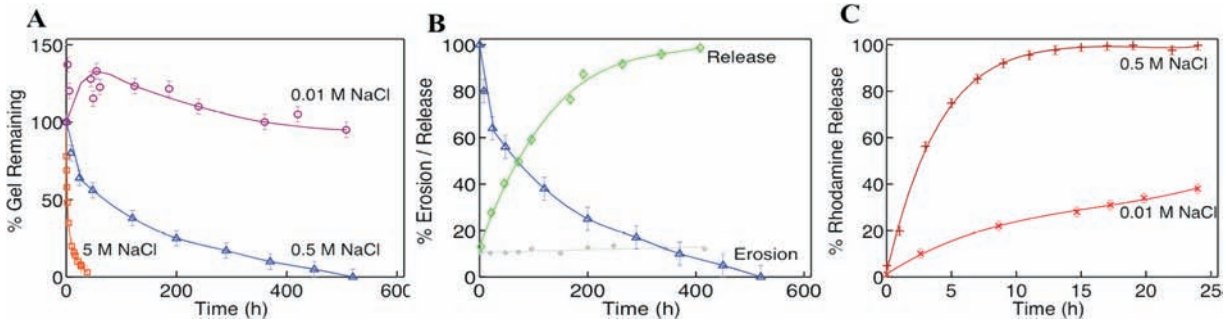

Figure 3. Erosion and content release by TPR smart gels. (A) A piece of gel was placed into a solution of 0.01 M sodium phosphate, pH 7.4, at different ionic strengths and 25 °C, and removed and weighed at various times following immersion. The percent gel mass remaining is plotted versus time for the different ionic strength solutions. (B) An aliquot of fluorescent protein (mVFP) or (C) the small molecule rhodamine (MW 422 Da) was entrapped during gelation. The release of entrapped molecule was monitored as a function of time, following the increase in fluorescence of the solution in which the gel was immersed. These measurements were made in Dulbecco/Vogt modified Eagle's minimal essential medium (DMEM), a commonly used tissue culture medium, which has an ionic strength of 166 mM, pH 7.4, at 37 °C. Release of the 26 kDa mVFP protein from the gel clearly mirrors gel erosion. Note that there is virtually no release in the 30 mM ionic strength solution (gray circles). (C) Data are shown for 0.01 M sodium phosphate, pH 7.4, plus 0.01 M NaCl (light red) or 0.5 M NaCl (dark red) at 25 °C. Release of rhodamine is far more rapid than the erosion of the gel. The lines through the points in all plots are included as a guide for the eye.

smart gels to sequester and release content, we included a fluorescent protein, mVFP (26 kDa), in the gelation mixture.[31] The resulting gels fully encapsulate the protein in a functional state, indicated by its fluorescence. The gels show negligible leakage of the protein when immersed for weeks in a solution of low ionic strength. When placed in a solution of higher ionic strength, however, the fluorescent protein is released, and the kinetics of release directly mirrors the kinetics of gel erosion (Figure 3B). Such deliberate, stimuli-responsive release is well-suited to possible application of these materials as protein or nucleic acid delivery devices.

We also studied the entrapment and release of small "drug mimetic" molecules by these gels. We encapsulated the fluorescent molecule, rhodamine (MW 422 Da), by including it in the gelation mix. The release of rhodamine is more rapid than the release of mVFP but is also facilitated by increasing the ionic strength of the solution. However, in this case release precedes gel erosion (Figure 3C). The difference in release behavior for mVFP and rhodamine is most simply rationalized by the relative sizes of these molecules; however, the interactions between TPR and mVFP proteins may also play a role.

In summary, we have fabricated ionic-strength-responsive hydrogels by using modular bottom-up protein design. These gels are cross-linked by specific, noncovalent interactions between repeat protein modules and their partner peptide ligands. The ability of the gels to encapsulate and release both large and small molecules bodes well for their potential use in controlled drug delivery applications. The robust elastic modulus and extraordinary elasticity of these gels suggests that, with application-specific optimization, these gels will be well-suited for cell culture and tissue engineering applications. Although we have presented the characterization of just one example of this type of smart gel design, the combination of modular TPR structure, specific and predictable self-assembly, and versatility of functionalization makes this approach a compelling path toward realizing new multifunctional materials with an array of tunable properties.

Acknowledgment. The authors thank members of the Regan group for critical discussions and reading of the manuscript and Kevin Lai for help in the preparation of Figure 1. This work was supported by the grants NIH GM 080515 and HFSP RGP44/2007 (LR), NSF CAREER Grant CBET-0547294 (E.R.D.), and NSF CBET-0828905 grant (C.O.O.).

Supporting Information Available: Experimental details. This material is available free of charge via the Internet at http://pubs.acs.org.

References

(1) Banwell, E. F.; Abelardo, E. S.; Adams, D. J.; Birchall, M. A.; Corrigan, A.; Donald, A. M.; Kirkland, M.; Serpell, L. C.; Butler, M. F.; Woolfson, D. N. *Nat. Mater.* **2009**, *8*, 596–600.
(2) Jia, X.; Kiick, K. L. *Macromol. Biosci.* **2009**, *9*, 140–156.
(3) Maskarinec, S. A.; Tirrell, D. A. *Curr. Opin. Biotechnol.* **2005**, *16*, 422–426.
(4) Petka, W. A.; Harden, J. L.; McGrath, K. P.; Wirtz, D.; Tirrell, D. A. *Science* **1998**, *281*, 389–392.
(5) Rajagopal, K.; Lamm, M. S.; Haines-Butterick, L. A.; Pochan, D. J.; Schneider, J. P. *Biomacromolecules* **2009**, *10*, 2619–2625.
(6) Sengupta, D.; Heilshorn, S. C. *Tissue Eng. Part B: Rev.* **2010**, *16*, 285–293.
(7) Shen, W.; Zhang, K.; Kornfield, J. A.; Tirrell, D. A. *Nat. Mater.* **2006**, *5*, 153–158.
(8) Topp, S.; Prasad, V.; Cianci, G. C.; Weeks, E. R.; Gallivan, J. P. *J. Am. Chem. Soc.* **2006**, *128*, 13994–13995.
(9) Wong Po Foo, C. T.; Lee, J. S.; Mulyasasmita, W.; Parisi-Amon, A.; Heilshorn, S. C. *Proc. Natl. Acad. Sci. U.S.A.* **2009**, *106*, 22067–22072.
(10) Branco, M. C.; Schneider, J. P. *Acta Biomater.* **2009**, *5*, 817–831.
(11) D'Andrea, L.; Regan, L. *Trends Biochem. Sci.* **2003**, *28*, 655–662.
(12) Scheufler, C.; Brinker, A.; Bourenkov, G.; Pegoraro, S.; Moroder, L.; Bartunik, H.; Hartl, F. U.; Moarefi, I. *Cell* **2000**, *101*, 199–210.
(13) Cortajarena, A. L.; Lois, G.; Sherman, E.; O'Hern, C. S.; Regan, L.; Haran, G. *J. Mol. Biol.* **2008**, *382*, 203–212.
(14) Cortajarena, A. L.; Regan, L. *Protein Sci.* **2006**, *15*, 1193–1198.
(15) Kajander, T.; Cortajarena, A. L.; Main, E. R.; Mochrie, S. G.; Regan, L. *J. Am. Chem. Soc.* **2005**, *127*, 10188–10190.
(16) Kajander, T.; Cortajarena, A. L.; Mochrie, S.; Regan, L. *Acta Crystallogr. D: Biol. Crystallogr.* **2007**, *63*, 800–811.
(17) Cortajarena, A. L.; Liu, T. Y.; Hochstrasser, M.; Regan, L. *ACS Chem. Biol.* **2010**, *5*, 545–552.
(18) Cortajarena, A. L.; Wang, J.; Regan, L. *FEBS J.* **2010**, *277*, 1058–1066.
(19) Cortajarena, A. L.; Yi, F.; Regan, L. *ACS Chem. Biol.* **2008**, *3*, 161–166.
(20) Grove, T. Z.; Hands, M.; Regan, L. *Protein Eng. Des. Sel.* **2010**, *23*, 449–455.
(21) Jackrel, M. E.; Cortajarena, A. L.; Liu, T. Y.; Regan, L. *ACS Chem. Biol.* **2010**, *5*, 553–562.
(22) Jackrel, M. E.; Valverde, R.; Regan, L. *Protein Sci.* **2009**, *18*, 762–774.
(23) Lutolf, M. P.; Hubbell, J. A. *Biomacromolecules* **2003**, *4*, 713–722.
(24) Yamaguchi, N.; Kiick, K. L. *Biomacromolecules* **2005**, *6*, 1921–1930.
(25) Dasgupta, B. R.; Weitz, D. A. *Phys. Rev. E: Stat. Nonlin. Soft Matter Phys.* **2005**, *71*, 021504–021602.
(26) Yan, C.; Pochan, D. J. *Chem. Soc. Rev.* **2010**, *39*, 3528–3540.
(27) Fonkwe, L. G.; Narsimhan, G.; Cha, A. S. *Food Hydrocolloids* **2003**, *17*, 871–883.
(28) Kretsinger, J. K.; Haines, L. A.; Ozbas, B.; Pochan, D. J.; Schneider, J. P. *Biomaterials* **2005**, *26*, 5177–5186.
(29) Storm, C.; Pastore, J. J.; MacKintosh, F. C.; Lubensky, T. C.; Janmey, P. A. *Nature* **2005**, *435*, 191–194.
(30) Discher, D. E.; Janmey, P.; Wang, Y. L. *Science* **2005**, *310*, 1139–1143.
(31) Ilagan, R. P.; Rhoades, E.; Gruber, D. F.; Kao, H. T.; Pieribone, V. A.; Regan, L. *FEBS J.* **2010**, *277*, 1967–1978.

JA106619W